Science Advances
AAAS

advances.sciencemag.org/cgi/content/full/7/12/eabd4735/DC1

Supplementary Materials for

Nanotransfection-based vasculogenic cell reprogramming drives functional recovery in a mouse model of ischemic stroke

Luke R. Lemmerman, Maria H. H. Balch, Jordan T. Moore, Diego Alzate-Correa, Maria A. Rincon-Benavides, Ana Salazar-Puerta, Surya Gnyawali, Hallie N. Harris, William Lawrence, Lilibeth Ortega-Pineda, Lauren Wilch, Ian B. Risser, Aidan J. Maxwell, Silvia Duarte-Sanmiguel, Daniel Dodd, Gina P. Guio-Vega, Dana M. McTigue, W. David Arnold, Shahid M. Nimjee, Chandan K. Sen, Savita Khanna, Cameron Rink, Natalia Higuita-Castro*, Daniel Gallego-Perez*

*Corresponding author. Email: gallegoperez.1@osu.edu (D.G.-P.); higuitacastro.1@osu.edu (N.H.-C.)

Published 19 March 2021, *Sci. Adv.* **7**, eabd4735 (2021)
DOI: 10.1126/sciadv.abd4735

This PDF file includes:

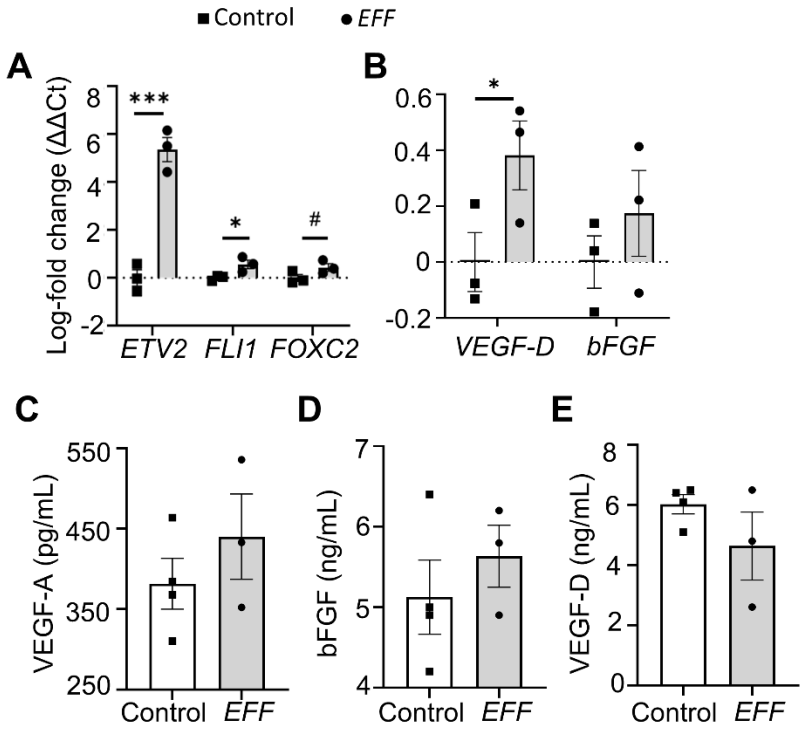

Supplementary Figure 1. Gene and protein expression profile of fibroblast post nanotransfection with the *EFF* cocktail vs. sham/control fibroblasts. qRT-PCR analysis of (**A**) *EFF* and (**B**) pro-lymphogenic/angiogenic factors in *EFF*-nanotransfected pMEFs at day 7 (n=3). The decrease in expression compared to day 1 readings is presumably due to the combined effect of iEC maturation, which may result in decreased expression of developmental transcription factors (*20*, *53*), and additional *in vitro* proliferation of fibroblasts that did not reprogram. ELISA analysis of pro-angiogenic proteins, (**C**) VEGF-A and (**D**) bFGF and pro-lymphogenic protein, (**E**) VEGF-D in pMEFs 24 hours post-nanotransfection with *EFF* compared to control/sham plasmids (n=3-4). All error bars are shown as SE. $^{\#}p=0.054$, $*p<0.05$, $***p<0.001$ (One-tailed t-test).

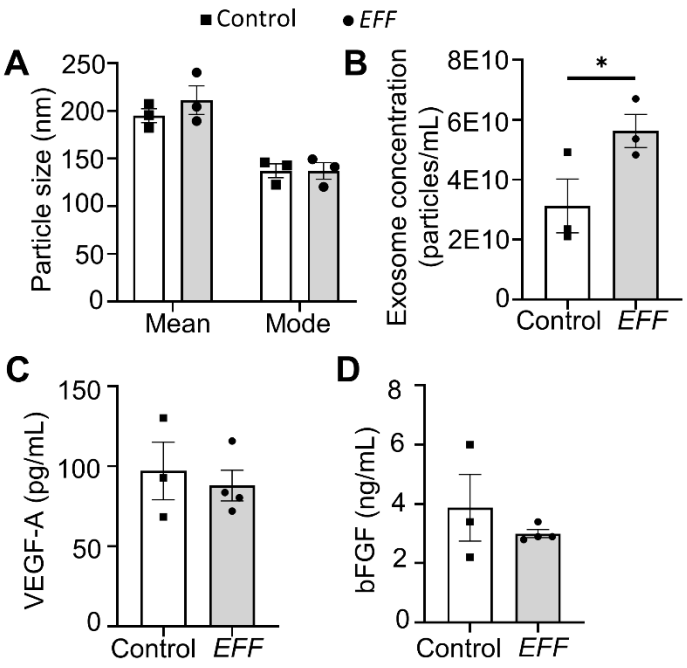

Supplementary Figure 2. Size and protein cargo characterization of exosomes secreted from fibroblast nanotransfected with the *EFF* cocktail vs. sham/control plasmids. (**A**) Size and (**B**) concentration profiles from exosomes collected from *EFF*-nanotransfected fibroblasts 24 hours post-nanotransfection compared to control (n=3). *EFF*-nanotransfected fibroblasts appeared to secrete more exosomes, but no significant changes in size were noted. ELISA analysis of pro-angiogenic proteins, (**C**) VEGF-A and (**D**) bFGF in exosomes collected from *EFF*-nanotransfected pMEFs 24 hours post-nanotransfection compared to control (n=3-4). No significant increase/trend was detected at the protein level. All error bars are shown as SE. *$p<0.05$ (One-tailed t-test).

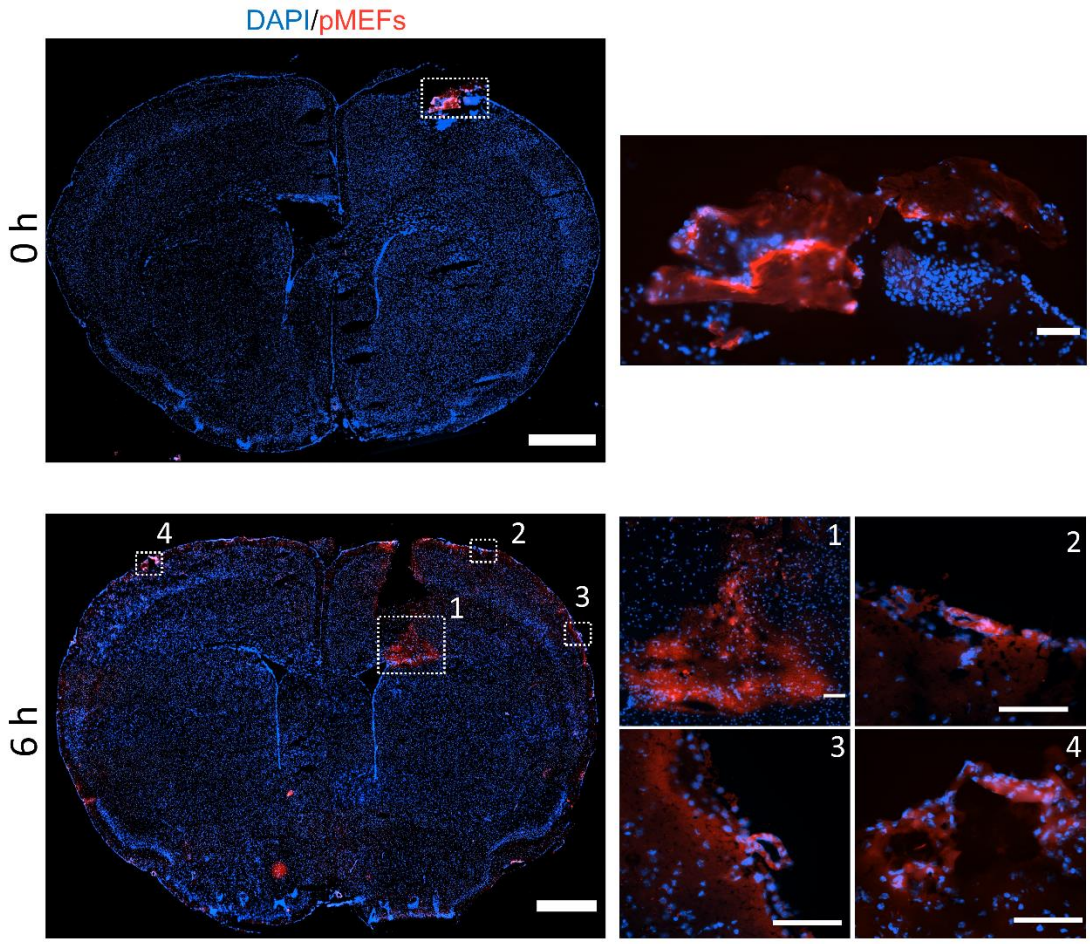

Supplementary Figure 3. Fibroblast location 0 and 6 hours after intracranial delivery in healthy mice. Fibroblasts were labelled with PKH26 (cell membrane marker; Sigma, ref. no. MKCK7206) immediately prior to intracranial delivery into the subarachnoid space in healthy mice. Representative fluorescence micrographs showing nuclear (DAPI) and labelled fibroblasts (PKH26) (**A**) immediately and (**B**) 6 hours post intracranial injection in healthy mice (scale bar = 1 mm for both whole brain images and 100 μm for all insets). These data indicate that after a few hours, the injected fibroblasts are prone to spreading along the cortex, crossing into the contralateral hemisphere, possibly aided by cerebrospinal fluid flow (*24*, *25*).

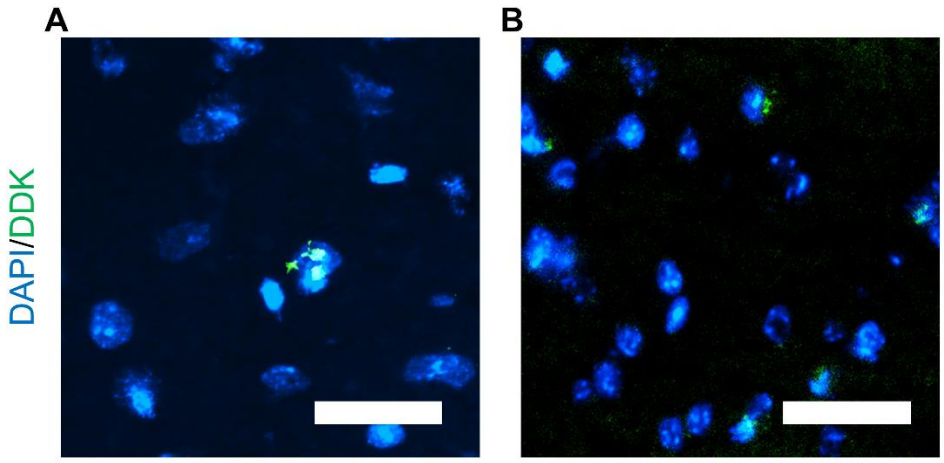

Supplementary Figure 4. Positive DDK immunostaining is suggestive of the presence of *EFF*-nanotransfected/expressing fibroblasts in the contralateral hemisphere at days 7 and 14 post-injection. Histological analysis for the DDK tag (green) on the *EFF* factors suggests that *EFF*-nanotransfected pMEFs can cross to the contralateral hemisphere following injection. This was verified in (**A**) brains that were not subjected to a stroke lesion (t = 7 days post-injection), as well as (**B**) brains that were subjected to a stroke lesion (t = 14 days post-injection) (scale bar = 25 μm).

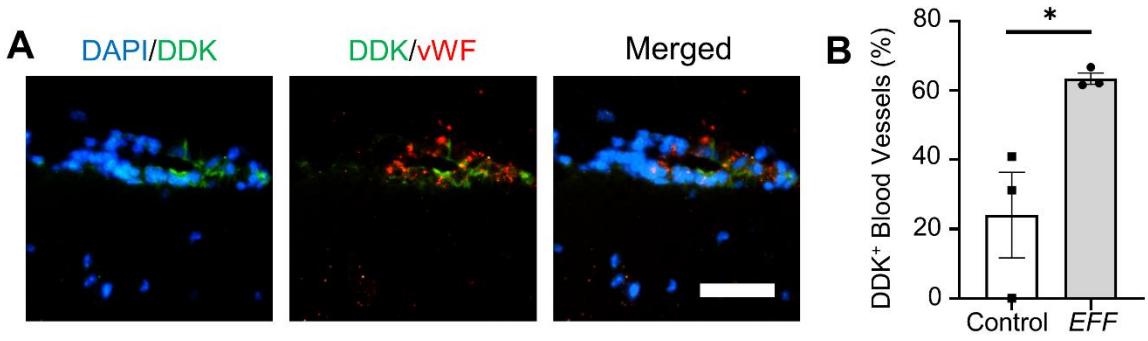

Supplementary Figure 5. *EFF*-nanotransfected fibroblasts observed to co-localize with brain vasculature after intracranial injection. (**A**) Fluorescence micrographs in the stroke-affected/ipsilateral hemisphere near the injection site 21 days post-stroke (*i.e.,* 14 days post-cell injection). The micrographs show cells that were immunoreactive for both the *EFF* tag (*i.e.,* DDK) and the endothelial cell marker vWF, presumably confirming the presence of *EFF*-nanotransfected pMEFs that converted into iECs, and that form integral/structural part of the newly developed iVas; (scale bar = 50 μm). (**B**) Quantification of DDK+ blood vessels near intracranial injection site (n=3). Notably, although significantly less than *EFF*-nanotransfected fibroblasts, some sham-nanotransfected fibroblasts also appear to be closely associated with vWF+ structures. This observation could potentially be indicative of vWF+ fibroblasts, which have been reported in previous studies when co-cultured in close proximity with endothelial cells (*54*), and/or simple physical proximity between the injected cells and pre-existing vasculature. All error bars are shown as SE. *$p<0.05$ (One-tailed t-test).

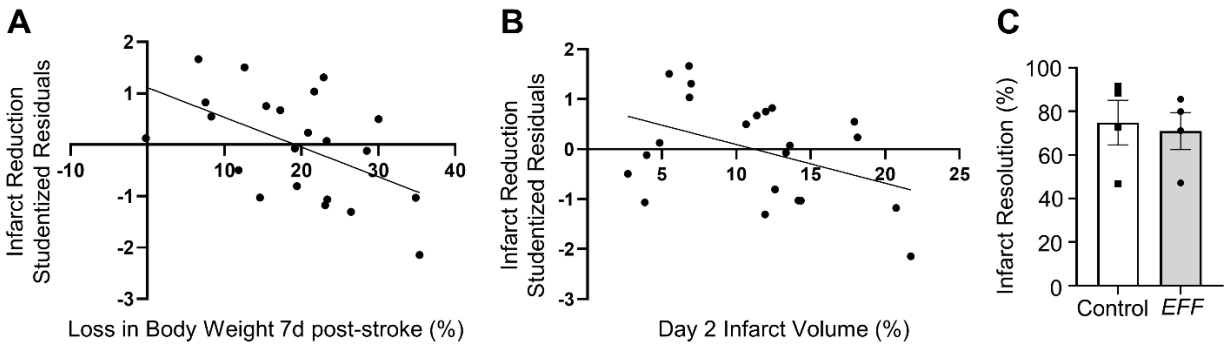

Supplementary Figure 6. Loss in body weight and day 2 infarct volume significantly impact infarct resolution. Linear regression analysis for infarct volume reduction confounding variables: **(A)** loss in body weight 7 days post-stroke ($R^2 = 0.268$, *adj.* $R^2 = 0.231$, *p-value = 0.014*, *n=22*) and **(B)** day-2 infarct volume ($R^2 = 0.174$, *adj.* $R^2 = 0.174$, *p-value = 0.054*, *n=22*). **(C)** Percent stroke volume reduction in mice with <17% loss in body weigh 7 days post-stroke (n=4). All error bars are shown as SE.

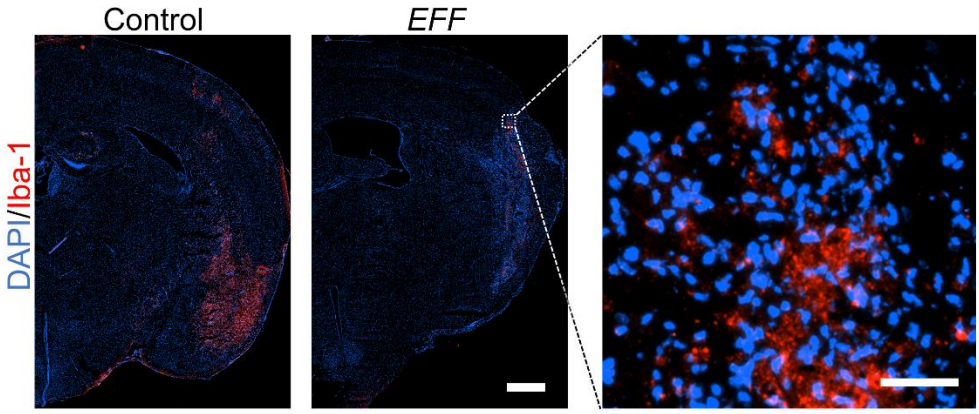

Supplementary Figure 7. Microglia presence in glial scar for mice treated with sham- and *EFF*-nanotransfected fibroblasts. Immunofluorescence micrographs of the ipsilateral hemisphere showing nuclear (DAPI) and microglia (Iba-1) staining 21 days post-stroke in mice treated with sham- or *EFF*-nanotransfected cells (scale bar = 750 μm) with representative higher magnification inset (scale bar = 50 μm).

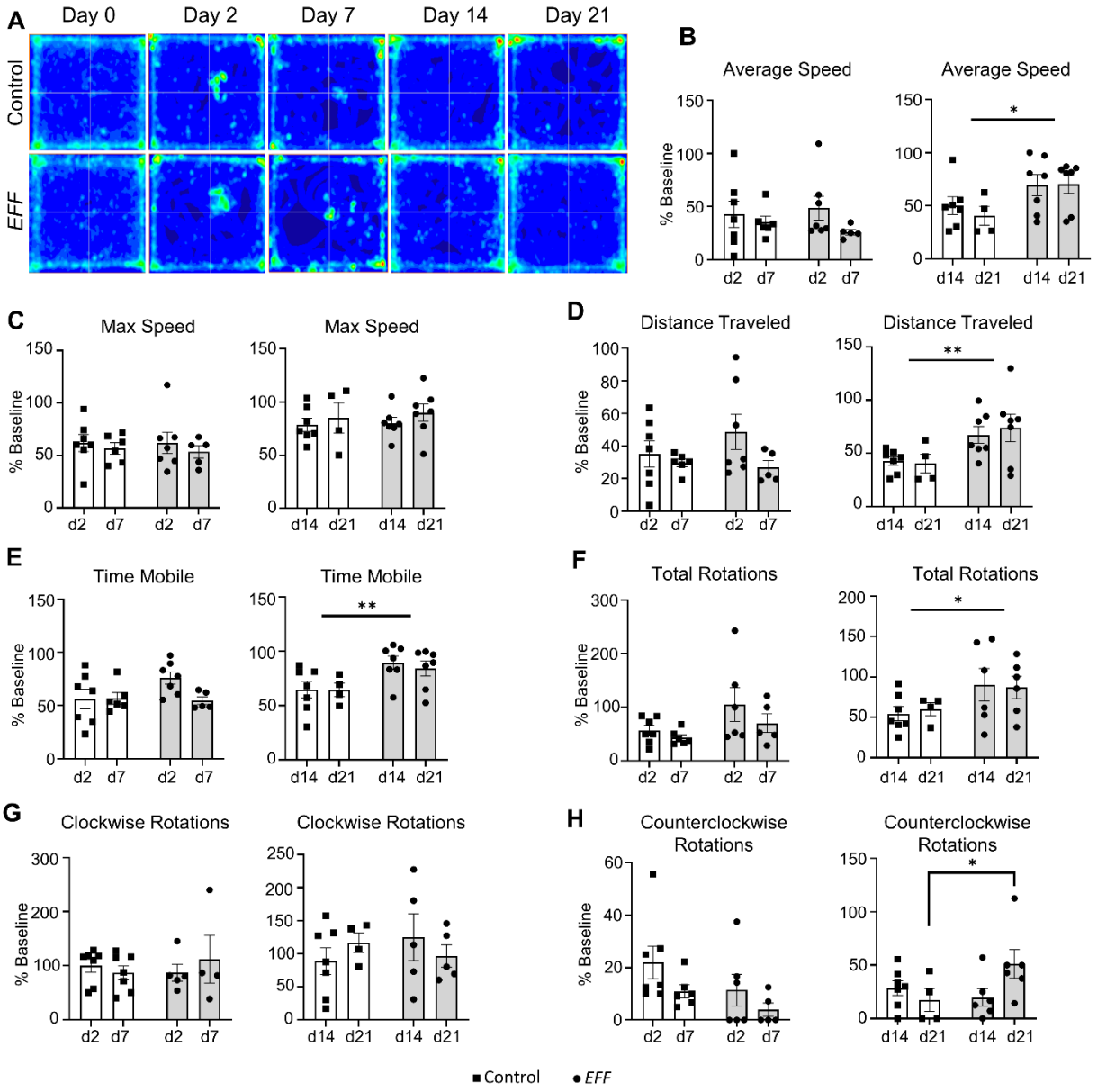

Supplementary Figure 8. Quantified parameters from open-field behavioral assessments throughout experimental timeline. **(A)** Occupancy heat maps depicting mice activity per location during behavioral testing on days 0, 2 ,7 ,14 and 21 post-stroke (dark blue – low activity area, red – high activity area). Individual behavioral parameter quantification (*left*) before and (*right*) after sham- or *EFF*-nanotransfected cell injection for **(B)** average speed, **(C)** maximum speed, **(D)** distance traveled, **(E)** time mobile, **(F)** total rotations, **(G)** clockwise rotations and **(H)**

counterclockwise rotations (n=4-7). All error bars are shown as SE. *$p<0.05$, **$p<0.01$, ***$p<0.001$ (two-way ANOVA)

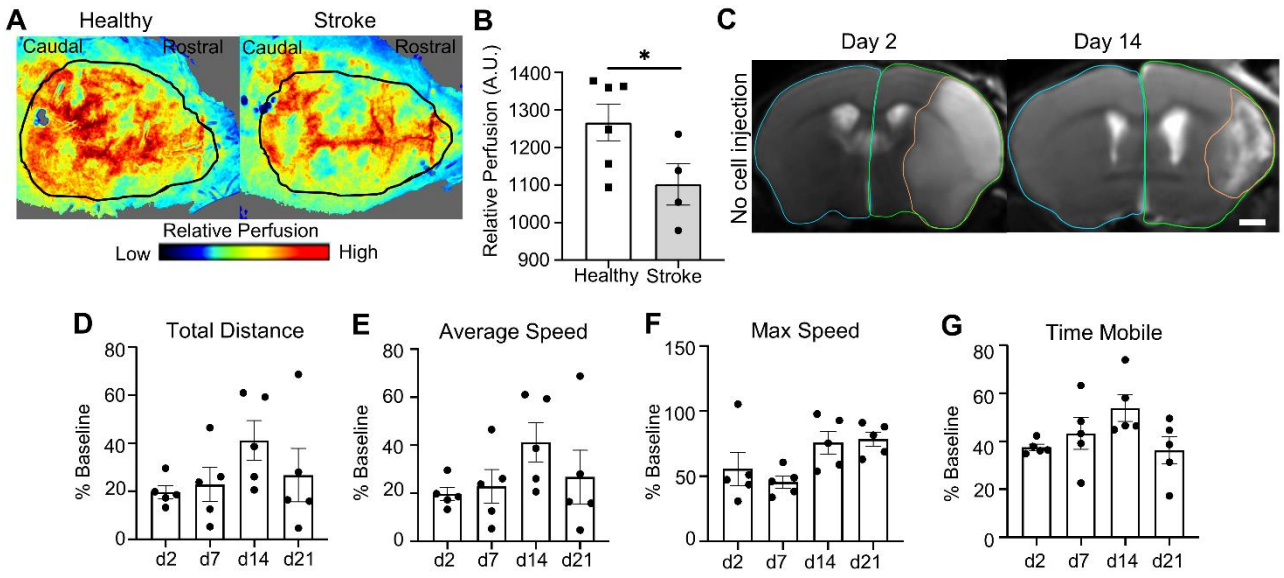

Supplementary Figure 9. Brain perfusion, infarct resolution and behavioral assessment in stroke-affected mice with no cell injection. A separate cohort of mice underwent the MCAO procedure without receiving the intracranial cell injection (*i.e.,* stroke only) to provide a reference group. (**A-B**) Brain perfusion in healthy mice or stroke only (21 days post-MCAO) with representative tracings for perfusion assessment (n=4-6). **(C)** T2-weighted MR images 2 days and 14 days post-stroke with representative tracings for assessment of infarct volume (orange) and hemisphere volumes (green/blue); (scale bar=1mm). Infarct resolution analysis for stroke only mice demonstrated a similar mean resolution of 49 percent (SE=7.9) from day 2 to day 14 post-stroke in stroke only mice (n=5) compared to mice intracranially injected with sham-nanotransfected pMEFs 7 days post-MCAO (mean resolution=47 percent, SE=8.8, n=7). Individual behavioral parameters were collected and quantified at pre-MCAO (baseline/day 0) and post-MCAO (days 2, 7, 14 and 21) for (**D**) distance traveled, (**E**) average speed, (**C**) maximum speed, (**D**) time mobile (n=5). Stroke only mice and mice treated with sham-nanotransfected pMEFs 7 days post-MCAO produced similar recovery trends with no/minimal marked increase in

distance travelled, average speed or time mobile parameters. All error bars are shown as SE. *$p<0.05$ (One-tailed t-test)

Supplementary Table 1. Full list of plasmid DNA vectors used in the study.

Plasmid vector	Company	Ref. Number	Type	Tag	Vector
pCMV6-Entry Tagged Cloning Vector (sham/control)	Origene	PS100001	N/A	Myc-DDK	pCMV6-Entry
Fli1 - Mouse friend leukemia integraion	Origene	MR225907	Mouse Tagged ORF Clone	Myc-DDK	pCMV6-Entry
ETV2 - Mouse ets variant gene 2	Origene	MR216258	Mouse Tagged ORF Clone	Myc-DDK	pCMV6-Entry
FoxC2 - Mouse forkhead box C2	Origene	MR221977	Mouse Tagged ORF Clone	Myc-DDK	pCMV6-Entry

Supplementary Table 2. Full list of primers used in the gene expression analysis in the study.

Gene Symbol	Gene Name	Gene Aliases	Species	Company	Ref. no.
Gapdh	glyceraldehyde-3-phosphate dehydrogenase	Gapd	Mouse	Thermofisher Scientific	Mm99999915_g1
Etv2	ets variant 2	Etsrp71	Mouse	Thermofisher Scientific	Mm00468389_m1
Fli1	Friend leukemia integration 1	EWSR2, Fli-1, SIC-1, Sic1	Mouse	Thermofisher Scientific	Mm00484410_m1
Foxc2	forkhead box C2	Fkh14, Hfhbf3, MFH-1, Mfh1	Mouse	Thermofisher Scientific	Mm00546194_s1
Figf	c-fos induced growth factor	AI325264, VEGF-D, Vegfd	Mouse	Thermofisher Scientific	Mm01131929_m1
Fgf2	fibroblast growth factor 2	Fgf-2, Fgfb, bFGF	Mouse	Thermofisher Scientific	Mm00433287_m1

Supplementary Table 3. Full list of immunohistology antibodies/proteins used in the study.

Target	Primary Antibody/Protein	Raised in	Company	ref. no.	Conc.	Secondary Antibody/Fluorofore	Conc.
Mature Neurons	NeuN	Rabbit	Abcam	ab177487	1:500	Goat α-rabbit IgG (H+L) (568)	1:200
Astroglia	GFAP	Rabbit	Abcam	ab7260	1:500	Goat α-rabbit IgG (H+L) (568)	1:200
Microglia	Iba1	Rabbit	Abcam	ab178846	1:500	Goat α-rabbit IgG (H+L) (568)	1:200
Endothelial cells	vWF	Rabbit	Abcam	ab6994	1:1000	Goat α-rabbit IgG (H+L) (568)	1:200
Endothelial cells	CD31	Rat	BD Pharmigen	550274	1:50	Goat α-rat IgG (H+L) (488)	1:200
Endothelial cells	RCA I (Lectin)	N/A	Vector	FL-1081	1:20	Fluorescein (conjugated w/ RCA I)	N/A
Plasmid tag	DDK	Mouse	Origene	TA50011	1:500	Goat α-mouse IgG (H+L) (488)	1:200

Supplementary Table 4. Full list of one-tailed t-test results.

Data	Statistical Test	Sham n	EFF n	Shapiro-Wilk Normality Test	Brown–Forsythe Equal Variance Test	T Statistic	p-value	DOF
Etv2 gene expression (cells 1 day post-NEP)	One-tailed Welch's t-test	3	3	Passed	Failed	-15.947	0.001	2.269
Fli1 gene expression (cells 1 day post-NEP)	One-tailed Student's t-test	3	3	Passed	Passed	-42.855	<0.001	4.000
FoxC2 gene expression (cells 1 day post-NEP)	One-tailed Student's t-test	3	3	Passed	Passed	-81.768	<0.001	4.000
VegfD gene expression (cells 1 day post-NEP)	One-tailed Welch's t-test	3	3	Passed	Failed	-4.589	0.021	2.037
bFGF gene expression (cells 1 day post-NEP)	One-tailed Student's t-test	3	3	Passed	Passed	-2.442	0.036	4.000
Etv2 gene expression (cells 7 day post-NEP)	One-tailed Student's t-test	3	3	Passed	Passed	-8.841	<0.001	4.000
Fli1 gene expression (cells 7 day post-NEP)	One-tailed Student's t-test	3	3	Passed	Passed	-2.978	0.020	4.000
FoxC2 gene expression (cells 7 day post-NEP)	One-tailed Student's t-test	3	3	Passed	Passed	-2.061	0.054	4.000
VegfD gene expression (cells 7 day post-NEP)	One-tailed Student's t-test	3	3	Passed	Passed	-2.356	0.039	4.000
bFGF gene expression (cells 7 day post-NEP)	One-tailed Student's t-test	3	3	Passed	Passed	-0.972	0.193	4.000
Etv2 gene expression (Exosomes 1 day post-NEP)	One-tailed Student's t-test	6	3	Passed	Passed	-10.327	<0.001	7.000
Fli1 gene expression (Exosomes 1 day post-NEP)	One-tailed Student's t-test	6	3	Passed	Passed	-12.134	<0.001	7.000
FoxC2 gene expression (Exosomes 1 day post-NEP)	One-tailed Student's t-test	6	3	Passed	Passed	-12.988	<0.001	7.000
VegfD gene expression (Exosomes 1 day post-NEP)	One-tailed Student's t-test	6	6	Passed	Passed	-0.727	0.242	10.000
bFGF gene expression (Exosomes 1 day post-NEP)	One-tailed Student's t-test	6	6	Passed	Passed	-1.450	0.089	10.000
Infarct Volume Resolution - all mice	One-tailed Student's t-test	11	11	Passed	Passed	-1.238	0.115	20.000
Infarct Volume Resolution - mice >17%BW loss	One-tailed Student's t-test	7	7	Passed	Passed	1.796	0.049	12.000
Infarct Volume Resolution - mice <17%BW loss	One-tailed Student's t-test	4	4	Passed	Passed	-0.291	0.390	6.000
CD31 Immunohistology - Ipsilateral hemisphere	One-tailed Student's t-test	6	8	Passed	Passed	-2.726	0.009	12.000
CD31 Immunohistology - Contralateral hemisphere	One-tailed Student's t-test	6	8	Passed	Passed	-2.275	0.021	12.000
Lectin immunohistology - Ipsilateral hemisphere	One-tailed Welch's t-test	4	7	Passed	Failed	-3.979	0.002	8.369
Lectin Immunohistology - Contralateral hemisphere	One-tailed Student's t-test	4	7	Passed	Passed	-2.725	0.012	9.000

NeuN Immunohistology - Ipsilateral hemisphere	One-tailed Student's t-test	8	9	Passed	Passed	-2.818	0.006	15.000
GFAP Immunohistology - Ipsilateral hemisphere	One-tailed Student's t-test	10	10	Passed	Passed	-2.373	0.015	18.000
DDK/vWF Immunohistology - Ipsilareral hemisphere	One-tailed Student's t-test	3	3	Passed	Passed	-3.162	0.017	4.000
Exosome mean particle size	One-tailed Student's t-test	3	3	Passed	Passed	0.971	0.193	4.000
Exosome mode particle size	One-tailed Student's t-test	3	3	Passed	Passed	-0.018	0.493	4.000
Exosome concentration	One-tailed Student's t-test	3	3	Passed	Passed	2.367	0.039	4.000
LSI - Healthy CI	One-tailed Student's t-test	6	6	Passed	Passed	-2.152	0.028	10.000
VEGF-A protein expression (cells 1 day post-NEP)	One-tailed Student's t-test	4	3	Passed	Passed	-1.009	0.180	5.000
VEGF-D protein expression (cells 1 day post-NEP)	One-tailed Welch's t-test	4	3	Passed	Failed	1.186	0.171	2.324
bFGF protein expression (cells 1 day post-NEP)	One-tailed Student's t-test	4	3	Passed	Passed	-0.803	0.229	5.000
VEGF-A protein expression (exosomes 1 day post-NEP)	One-tailed Student's t-test	3	4	Passed	Passed	0.485	0.324	5.000
bFGF protein expression (exosomes 1 day post-NEP)	One-tailed Welch's t-test	3	4	Passed	Failed	0.767	0.261	2.058
LSI - Healthy(H) /stroke(S) only	One-tailed Student's t-test	(H)6	(S)4	Passed	Passed	2.183	0.030	8.000

Supplementary Table 5. Full list of two-way ANOVA results.

Data	Statistical Test	Sham n	EFF n	Normality Test	Equal Variance Test	T: F statistic	T: p-value	D: F statistic	D: p-value	TDI: F statistic	TDI: p-value
d14 and d21 Behavioral - Average Speed	Two-way ANOVA	d14=7; d21=4	d14=7; d21=7	Passed	Passed	6.736	0.017	0.213	0.650	0.304	0.587
d14 and d21 Behavioral - Max Speed	Two-way ANOVA	d14=7; d21=4	d14=7; d21=7	Passed	Passed	0.158	0.695	0.984	0.333	0.046	0.832
d14 and d21 Behavioral - Distance Traveled	Two-way ANOVA	d14=7; d21=4	d14=7; d21=7	Passed	Passed	9.331	0.006	0.051	0.823	0.218	0.645
d14 and d21 Behavioral - Time Mobile	Two-way ANOVA on Ranks	d14=7; d21=4	d14=7; d21=7	Failed	Passed	11.584	0.003	2.339	0.141	0.456	0.507
d14 and d21 Behavioral - # of Total Rotations	Two-way ANOVA	d14=7; d21=4	d14=7; d21=6	Passed	Passed	4.638	0.044	0.007	0.935	0.094	0.762
d14 and d21 Behavioral - # of Clockwise Rotations	Two-way ANOVA on Ranks	d14=7; d21=4	d14=6; d21=5	Passed	Failed	0.033	0.859	1.138	0.301	1.190	0.290
d14 and d21 Behavioral - # of Counterclockwise Rotations	Two-way ANOVA	d14=7; d21=4	d14=7; d21=6	Passed	Passed	1.507	0.235	0.986	0.333	4.413	0.049*
d2 and d7 Behavioral - Average Speed	Two-way ANOVA	d2=7; d7=6	d2=7; d7=5	Passed	Passed	0.028	0.869	2.260	0.148	0.559	0.463
d2 and d7 Behavioral - Max Speed	Two-way ANOVA	d2=7; d7=6	d2=7; d7=5	Passed	Passed	0.036	0.851	0.695	0.414	0.045	0.834
d2 and d7 Behavioral - Distance Traveled	Two-way ANOVA	d2=7; d7=6	d2=7; d7=5	Passed	Passed	0.463	0.504	2.952	0.100	1.062	0.314
d2 and d7 Behavioral - Time Mobile	Two-way ANOVA	d2=7; d7=6	d2=7; d7=5	Passed	Passed	1.628	0.216	2.315	0.143	2.562	0.124
d2 and d7 Behavioral - # of Total Rotations	Two-way ANOVA on Ranks	d2=7; d7=6	d2=6; d7=5	Failed	Passed	2.497	0.130	0.452	0.509	0.009	0.927
d2 and d7 Behavioral - # of Clockwise Rotations	Two-way ANOVA	d2=7; d7=7	d2=5; d7=4	Passed	Passed	0.090	0.768	0.085	0.774	0.901	0.354
d2 and d7 Behavioral - # of Counterclockwise Rotations	Two-way ANOVA on Ranks	d2=7; d7=6	d2=5; d7=5	Failed	Passed	2.030	0.170	0.135	0.717	0.357	0.557

Legend: Treatment = T; Day = D; Treatment x Day Interaction = TDI; Normality Test = Shapiro-Wilk Test; Equal Variance = Brown-Forsythe Test	*	Interaction	T-statistic	p-value
		Treatmentxd21	2.197	0.041

REFERENCES AND NOTES

1. W. Johnson, O. Onuma, M. Owolabi, S. Sachdev, Stroke: A global response is needed. *Bull. World Health Organ.* **94**, 634 (2016).
2. S. S. Virani, A. Alonso, E. J. Benjamin, M. S. Bittencourt, C. W. Callaway, A. P. Carson, A. M. Chamberlain, A. R. Chang, S. Cheng, F. N. Delling, L. Djousse, M. S. V. Elkind, J. F. Ferguson, M. Fornage, S. S. Khan, B. M. Kissela, K. L. Knutson, T. W. Kwan, D. T. Lackland, T. T. Lewis, J. H. Lichtman, C. T. Longenecker, M. S. Loop, P. L. Lutsey, S. S. Martin, K. Matsushita, A. E. Moran, M. E. Mussolino, A. M. Perak, W. D. Rosamond, G. A. Roth, U. K. A. Sampson, G. M. Satou, E. B. Schroeder, S. H. Shah, C. M. Shay, N. L. Spartano, A. Stokes, D. L. Tirschwell, L. B. VanWagner, C. W. Tsao; American Heart Association Council on Epidemiology and Prevention Statistics Committee and Stroke Statistics Subcommittee, Heart disease and stroke statistics—2020 update: A report from the american heart association. *Circulation* **141**, CIR0000000000000757 (2020).
3. National Institute of Neurological Disorders and Stroke rt-PA Stroke Study Group, Tissue plasminogen activator for acute ischemic stroke. *N. Eng. J. Med.* **333**, 1581–1588 (1995).
4. R. G. Nogueira, A. P. Jadhav, D. C. Haussen, A. Bonafe, R. F. Budzik, P. Bhuva, D. R. Yavagal, M. Ribo, C. Cognard, R. A. Hanel, C. A. Sila, A. E. Hassan, M. Millan, E. I. Levy, P. Mitchell, M. Chen, J. D. English, Q. A. Shah, F. L. Silver, V. M. Pereira, B. P. Mehta, B. W. Baxter, M. G. Abraham, P. Cardona, E. Veznedaroglu, F. R. Hellinger, L. Feng, J. F. Kirmani, D. K. Lopes, B. T. Jankowitz, M. R. Frankel, V. Costalat, N. A. Vora, A. J. Yoo, A. M. Malik, A. J. Furlan, M. Rubiera, A. Aghaebrahim, J.M. Olivot, W. G. Tekle, R. Shields, T. Graves, R. J. Lewis, W. S. Smith, D. S. Liebeskind, J. L. Saver, T. G. Jovin, Thrombectomy 6 to 24 hours after stroke with a mismatch between deficit and infarct. *N. Eng. J. Med.* **378**, 11–21 (2018).
5. W. Hacke, M. Kaste, E. Bluhmki, M. Brozman, A. Dávalos, D. Guidetti, V. Larrue, K. R. Lees, Z. Medeghri, T. Machnig, D. Schneider, Rüdiger von Kummer, N. Wahlgren, D. Toni; ECASS Investigators, Thrombolysis with alteplase 3 to 4.5 hours after acute ischemic stroke. *N. Eng. J. Med.* **359**, 1317–1329 (2008).
6. M. Krause, T. G. Phan, C. G. Sobey, H. Ma, R. Lim, Cell-based therapies for stroke: Are we there yet? *Front. Neurol.* **10**, 656 (2019).
7. L. Fletcher, S. Kohli, S. M. Sprague, R. A. Scranton, S. A. Lipton, A. Parra, D. F. Jimenez, M. Digicaylioglu, Intranasal delivery of erythropoietin plus insulin-like growth factor–I for acute neuroprotection in stroke. *J. Neurosurg.* **111**, 164–170 (2009).

8. J. Silver, J. H. Miller, Regeneration beyond the glial scar. *Nat. Rev. Neurosci.* **5**, 146–156 (2004).
9. L.-R. Zhao, A. Willing, Enhancing endogenous capacity to repair a stroke-damaged brain: An evolving field for stroke research. *Prog. Neurobiol.* **163-164**, 5–26 (2018).
10. P. R. Thored, J. Wood, A. Arvidsson, J. Cammenga, Z. Kokaia, O. Lindvall, Long-term neuroblast migration along blood vessels in an area with transient angiogenesis and increased vascularization after stroke. *Stroke* **38**, 3032–3039 (2007).
11. R. Tamarat, J. S. Silvestre, S. le Ricousse-Roussanne, V. Barateau, L. Lecomte-Raclet, M. Clergue, M. Duriez, G. Tobelem, B. I. Lévy, Impairment in ischemia-induced neovascularization in diabetes: Bone marrow mononuclear cell dysfunction and therapeutic potential of placenta growth factor treatment. *Am. J. Pathol.* **164**, 457–466 (2004).
12. M. Rodrigues, V. W. Wong, R. C. Rennert, C. R. Davis, M. T. Longaker, G. C. Gurtner, Progenitor cell dysfunctions underlie some diabetic complications. *Am. J. Pathol.* **185**, 2607–2618 (2015).
13. A. S. Lee, C. Tang, M. S. Rao, I. L. Weissman, J. C. Wu, Tumorigenicity as a clinical hurdle for pluripotent stem cell therapies. *Nat. Med.* **19**, 998–1004 (2013).
14. T. Vierbuchen, M. Wernig, Direct lineage conversions: Unnatural but useful? *Nat. Biotechnol.* **29**, 892–907 (2011).
15. H. Okano, M. Nakamura, K. Yoshida, Y. Okada, O. Tsuji, S. Nori, E. Ikeda, S. Yamanaka, K. Miura, Steps toward safe cell therapy using induced pluripotent stem cells. *Circ. Res.* **112**, 523–533 (2013).
16. A. J. Mellott, M. L. Forrest, M. S. Detamore, Physical non-viral gene delivery methods for tissue engineering. *Ann. Biomed. Eng.* **41**, 446–468 (2013).
17. P. E. Boukany, A. Morss, W.C. Liao, B. Henslee, H.C. Jung, X. Zhang, B. Yu, X. Wang, Y. Wu, L. Li, K. Gao, X. Hu, X. Zhao, O. Hemminger, W. Lu, G. P. Lafyatis, L. J. Lee, Nanochannel electroporation delivers precise amounts of biomolecules into living cells. *Nat. Nanotechnol.* **6**, 747–754 (2011).
18. D. Gallego-Perez, J. J. Otero, C. Czeisler, J. Ma, C. Ortiz, P. Gygli, F. P. Catacutan, H.N. Gokozan, A. Cowgill, T. Sherwood, S. Ghatak, V. Malkoc, X. Zhao, W. C. Liao, S. Gnyawali, X. Wang, A. F. Adler, K. Leong, B. Wulff, T.A. Wilgus, C. Askwith, S. Khanna, C. Rink, C.K. Sen, L. J. Lee, Deterministic transfection drives efficient nonviral reprogramming and uncovers reprogramming barriers. *Nanomedicine* **12**, 399–409 (2016).

19. D. Gallego-Perez, D. Pal, S. Ghatak, V. Malkoc, N. Higuita-Castro, S. Gnyawali, L. Chang, W.C. Liao, J. Shi, M. Sinha, K. Singh, E. Steen, A. Sunyecz, R. Stewart, J. Moore, T. Ziebro, R. G. Northcutt, M. Homsy, P. Bertani, W. Lu, S. Roy, S. Khanna, C. Rink, V. B. Sundaresan, J. J. Otero, L. J. Lee, C. K. Sen, Topical tissue nano-transfection mediates non-viral stroma reprogramming and rescue. *Nat. Nanotechnol.* **12**, 974–979 (2017).
20. S. Lee, T. A. Vuong, X. Wen, H. J. Jeong, H. K. So, I. Kwon, J. S. Kang, H. Cho, Methylation determines the extracellular calcium sensitivity of the leak channel NALCN in hippocampal dentate granule cells. *Exp. Mol. Med.* **51**, 1–14 (2019).
21. B. H. Dobkin, S. T. Carmichael, The specific requirements of neural repair trials for stroke. *Neurorehabil. Neural Repair* **30**, 470–478 (2016).
22. C. Iadecola, J. Anrather, The immunology of stroke: From mechanisms to translation. *Nat. Med.* **17**, 796–808 (2011).
23. N. G. Ordóñez, Immunohistochemical endothelial markers: A review. *Adv Anat Pathol* **19**, 281–295 (2012).
24. E. A. Salegio, H. Streeter, N. Dube, P. Hadaczek, L. Samaranch, A. P. Kells, W. S. Sebastian, Y. Zhai, J. Bringas, T. Xu, J. Forsayeth, K. S. Bankiewicz, Distribution of nanoparticles throughout the cerebral cortex of rodents and non-human primates: Implications for gene and drug therapy. *Front. Neuroanat.* **8**, 9 (2014).
25. B. Sweetman, A. A. Linninger, Cerebrospinal fluid flow dynamics in the central nervous system. *Ann. Biomed. Eng.* **39**, 484–496 (2011).
26. X. K. Zhang, D. K. Watson, The FLI-1 transcription factor is a short-lived phosphoprotein in T cells. *J. Biochem.* **137**, 297–302 (2005).
27. I. Loubinoux, A. Volk, J. Borredon, S. Guirimand, B. Tiffon, J. Seylaz, P. Méric, Spreading of vasogenic edema and cytotoxic edema assessed by quantitative diffusion and T2 magnetic resonance imaging. *Stroke* **28**, 419–427 (1997).
28. A.-C. Jönsson, I. Lindgren, B. Norrving, A. Lindgren, Weight loss after stroke: A population-based study from the Lund Stroke Register. *Stroke* **39**, 918–923 (2008).
29. S. D. Bouziana, K. Tziomalos, Malnutrition in patients with acute stroke. *J. Nutrit. Metab.* **2011**, 1–7 (2011).

30. A. Datta, D. Sarmah, L. Mounica, H. Kaur, R. Kesharwani, G. Verma, P. Veeresh, V. Kotian, K. Kalia, A. Borah, X. Wang, K. R. Dave, D. R. Yavagal, P. Bhattacharya, Cell death pathways in ischemic stroke and targeted pharmacotherapy. *Transl. Stroke Res.* **11**, 1185–1202 (2020).
31. N. R. Sims, W. P. Yew, Reactive astrogliosis in stroke: Contributions of astrocytes to recovery of neurological function. *Neurochem. Int.* **107**, 88–103 (2017).
32. L. Huang, Z. B. Wu, Q. ZhuGe, W. M. Zheng, B. Shao, B. Wang, F. Sun, K. Jin, Glial scar formation occurs in the human brain after ischemic stroke. *Int. J. Med. Sci.* **11**, 344–348 (2014).
33. M. Nedergaard, U. Dirnagl, Role of glial cells in cerebral ischemia. *Glia* **50**, 281–286 (2005).
34. G. Nys, M. J. E. van Zandvoort, P. L. M. de Kort, H. B. van der Worp, B. P. W. Jansen, A. Algra, E. H. F. de Haan, L. J. Kappelle, The prognostic value of domain-specific cognitive abilities in acute first-ever stroke. *Neurology* **64**, 821–827 (2005).
35. P. M. Pedersen, H. S. Jørgensen, H. Nakayama, H. O. Raaschou, T. S. Olsen, Hemineglect in acute stroke-incidence and prognostic implications: The Copenhagen Stroke Study1. *Am. J. Phys. Med. Rehabil.* **76**, 122–127 (1997).
36. J. Ringman, J. Saver, R. Woolson, W. Clarke, H. Adams, Frequency, risk factors, anatomy, and course of unilateral neglect in an acute stroke cohort. *Neurology* **63**, 468–474 (2004).
37. G. Gainotti, Les manifestations de negligence et d'inattention pour l'hemispace. *Cortex* **4**, 64–91 (1968).
38. L. Pizzamiglio, C. Bergego, P. Halligan, V. Homberg, I. Robertson, E. Weber, B. Wilson, P. Zoccolotti, G. Deloche, Factors affecting the clinical measurement of visuo-spatial neglect. *Behav. Neurol.* **5**, 233–240 (1992).
39. K. L. Schaar, M. M. Brenneman, S. I. Savitz, Functional assessments in the rodent stroke model. *Exp. Transl. Stroke Med.* **2**, 13 (2010).
40. T. Schallert, D. Adkins, *Primer on Cerebrovascular Diseases* (Elsevier, 2017), pp. 355–360.
41. Z. Fei, Y. Wu, S. Sharma, D. Gallego-Perez, N. Higuita-Castro, D. Hansford, J. J. Lannutti, L. J. Lee, Gene delivery to cultured embryonic stem cells using nanofiber-based sandwich electroporation. *Anal. Chem.* **85**, 1401–1407 (2013).
42. Y. Wu, M. C. Terp, K. J. Kwak, D. Gallego-Perez, S. P. Nana-Sinkam, L. J. Lee, Surface-mediated nucleic acid delivery by lipoplexes prepared in microwell arrays. *Small* **9**, 2358–2367 (2013).

43. N. Higuita-Castro, D. Gallego-Perez, K. Love, M. R. Sands, G. Kaletunç, D. J. Hansford, Soft lithography-based fabrication of biopolymer microparticles for nutrient microencapsulation. *Indust. Biotechnol.* **8**, 365–371 (2012).
44. L. Diaz-Starokozheva, D. Das, X. Gu, J. T. Moore, L. R. Lemmerman, I. Valerio, H. M. Powell, N. Higuita-Castro, M. R. Go, A. F. Palmer, D. Gallego-Perez, Early intervention in ischemic tissue with oxygen nanocarriers enables successful implementation of restorative cell therapies. *Cell. Mol. Bioeng.* **13**, 435–446 (2020).
45. J. T. Moore, C. G. Wier, L. R. Lemmerman, L. Ortega-Pineda, D. J. Dodd, W. R. Lawrence, S. Duarte-Sanmiguel, K. Dathathreya, L. Diaz-Starokozheva, H. N. Harris, C. K. Sen, I. L. Valerio, N. Higuita-Castro, W. D. Arnold, S. J. Kolb, D. Gallego-Perez, Nanochannel-based poration drives benign and effective nonviral gene delivery to peripheral nerve tissue. *Adv. Biosyst.* **4**, e2000157 (2020).
46. Y. Jin, J. S. Lee, J. Kim, S. Min, S. Wi, J. H. Yu, G.-E. Chang, A.-N. Cho, Y. Choi, D.-H. Ahn, S.-R. Cho, E. Cheong, Y.G. Kim, H.-P. Kim, Y. Kim, D. S. Kim, H. W. Kim, Z. Quan, H.-C. Kang, S.W. Cho, Three-dimensional brain-like microenvironments facilitate the direct reprogramming of fibroblasts into therapeutic neurons. *Nat. Biomed. Eng.* **2**, 522–539 (2018).
47. S.-J. Chen, C. M. Chang, S. K. Tsai, Y. L. Chang, S. J. Chou, S. S. Huang, L. K. Tai, Y. C. Chen, H. H. Ku, H. Y. Li, S. H. Chiou, Functional improvement of focal cerebral ischemia injury by subdural transplantation of induced pluripotent stem cells with fibrin glue. *Stem Cells Dev.* **19**, 1757–1767 (2010).
48. J. A. Stokum, V. Gerzanich, J. M. Simard, Molecular pathophysiology of cerebral edema. *J. Cereb. Blood Flow Metab.* **36**, 513–538 (2016).
49. A. Marmarou, A review of progress in understanding the pathophysiology and treatment of brain edema. *Neurosurg. Focus* **22**, E1 (2007).
50. I. Arnaoutova, H. K. Kleinman, In vitro angiogenesis: Endothelial cell tube formation on gelled basement membrane extract. *Nat. Protoc.* **5**, 628–635 (2010).
51. M. Königshoff, M. Kramer, N. Balsara, J. Wilhelm, O. V. Amarie, A. Jahn, F. Rose, L. Fink, W. Seeger, L. Schaefer, A. Günther, O. Eickelberg, WNT1-inducible signaling protein–1 mediates pulmonary fibrosis in mice and is upregulated in humans with idiopathic pulmonary fibrosis. *J. Clin. Invest.* **119**, 772–787 (2009).

52. J. Schindelin, I. Arganda-Carreras, E. Frise, V. Kaynig, M. Longair, T. Pietzsch, S. Preibisch, C. Rueden, S. Saalfeld, B. Schmid, J.-Y. Tinevez, D. J. White, V. Hartenstein, K. Eliceiri, P. Tomancak, A. Cardona, Fiji: an open-source platform for biological-image analysis. *Nat. Methods* **9**, 676–682 (2012).
53. S. De Val, B. L. Black, Transcriptional control of endothelial cell development. *Dev. Cell* **16**, 180–195 (2009).
54. J. Giddings, S. Hogg, I. Legg, I. Hughes, The relationship between von Willebrand factor antigen and fibronectin in human plasma, endothelial cells and fibroblasts in culture. *Thromb. Res.* **44**, 291–301 (1986).